

# TESTING HIGH DIMENSIONAL DIFFERENTIAL MATRICES, WITH APPLICATION TO DETECTING SCHIZOPHRENIA RISK GENES

BY LINGXUE ZHU<sup>\*</sup>, JING LEI<sup>\*</sup>, BERNIE DEVLIN<sup>†</sup> AND KATHRYN ROEDER<sup>\*</sup>

*Carnegie Mellon University<sup>\*</sup> and University of Pittsburgh<sup>†</sup>*

Scientists routinely compare gene expression levels in cases versus controls in part to determine genes associated with a disease. Similarly, detecting case-control differences in co-expression among genes can be critical to understanding complex human diseases; however statistical methods have been limited by the high dimensional nature of this problem. In this paper, we construct a sparse-Leading-Eigenvalue-Driven (sLED) test for high-dimensional differential matrices, defined as the difference of gene-gene “relationship” matrices in two populations. sLED encompasses the traditional two-sample covariance test as a special case, but it can also be applied to more general scenarios such as comparing weighted adjacency matrices. By focusing on the spectrum of the differential matrix, sLED provides a novel perspective that accommodates the sparse and weak signals in many gene expression data and is closely related with Sparse Principal Component Analysis. When testing two-sample high dimensional covariance matrices, sLED achieves full power asymptotically under mild assumptions, and simulation studies verify that it outperforms other existing procedures for many biologically plausible scenarios. Applying sLED to the largest gene-expression dataset comparing Schizophrenia and control brains, we provide a novel list of risk genes and reveal intriguing patterns in gene co-expression change for Schizophrenia subjects.

**1. Introduction.** High throughput technologies provide the capacity for measuring potentially interesting genetic features on the scale of tens of thousands. With the goal of understanding various complex human diseases, a widely used technique is gene differential expression analysis, which focuses on the marginal effect of each variant. Converging evidence has also revealed the importance of co-expression among genes, but analytic techniques are still underdeveloped. Improved methods in this domain will enhance our understanding of how complex disease affects the patterns of gene expression, shedding light on both the development of disease and its pathological consequences.

Schizophrenia (SCZ), a severe mental disorder with 0.7% lifetime risk [McGrath et al. (2008)], is one of the complex human traits that has been known for decades to be highly heritable but whose genetic etiology and pathological consequences remain unclear. What has been repeatedly confirmed is that a large proportion of SCZ liability traces to polygenetic variation involving many hundreds of genes together, with each variant exerting a small impact [Purcell et al. (2014); International Schizophrenia Consortium et al. (2009)]. Despite the large expected number, only a small fraction of risk loci have been conclusively identified [Schizophrenia

---

*Keywords and phrases:* Permutation test, high-dimensional data, covariance matrix, sparse principal component analysis.

Working Group of the Psychiatric Genomics Consortium (2014)]. This failure is mainly due to the limited signal strength of individual variants and under-powered mean-based association studies. Still, several biological processes, including synaptic mechanisms and glutamatergic neurotransmission, have been reported to be implicated in the risk for SCZ [Fromer et al. (2016)]. The observation that each genetic variant contributes only moderately to risk, and that each affected individual carries many risk variants, suggests that SCZ develops as a consequence of subtle alterations of both gene expression and co-expression, which requires development of statistical methods to describe the subtle, wide-spread co-expression differences.

Pioneering efforts have started in this direction. Very recently, the Common-Mind Consortium (CMC) completed a large-scale RNA sequencing on dorsolateral prefrontal cortex from 279 control and 258 SCZ subjects, forming the largest brain gene expression data set on SCZ [Fromer et al. (2016)]. Analyses of these data by the CommonMind Consortium suggest that many genes show altered expression between case and control subjects, although the mean differences are small. By combining gene expression and co-expression patterns with results from genetic association studies, it appears that genetic association signals tend to cluster in certain sets of tightly co-expressed genes, so called co-expression modules [Zhang and Horvath (2005)]. Still, the study of how gene co-expression patterns change from controls to SCZ subjects remains incomplete. Here, we address this problem using a hypothesis test that compares some gene co-expression and gene-gene “relationship” matrices between control and SCZ samples, with integrated variable selection.

Our testing framework encompasses the widely used two-sample covariance matrix test. This problem has been thoroughly studied in traditional multivariate analysis [Anderson et al. (1958)], but becomes nontrivial once we enter the high-dimensional regime. Previous high-dimensional covariance testing methods focus on either the  $L_2$ -type distance between matrices where all entries are considered [Srivastava and Yanagihara (2010); Li and Chen (2012)], or the  $L_\infty$ -type distance where only the largest deviation is utilized [Cai, Liu and Xia (2013); Chang, Zhou and Zhou (2015)]. These two lines of inquiries are designed for two extreme situations, respectively: when almost all genes exhibit some difference in co-expression patterns, or when there is one “leading” pair of genes whose co-expression pattern has an extraordinary deviation in two populations. However, the mechanism of SCZ is most likely to lie somewhere in between, where the difference may occur among hundreds of genes (compared to a total of  $\approx 20,000$  human genes), yet each deviation remains small. In other words, a two-sample covariance test that is designed for the sparse and weak alternative is needed. A recent paper opens this line of inquiry by exploring the use of random matrix projection [Wu and Li (2015)], but the power of their test is not well understood.

In this paper, we propose a sparse-Leading-Eigenvalue-Driven (sLED) test. It opens a novel perspective for matrix comparisons by evaluating the spectrum of the differential matrix, defined as the difference between two “relationship” matrices. This provides greater flexibility, power and insight for many biologically plausible models, including the situation where only a small cluster of genes have abnormalities in SCZ subjects, so that the differential matrix is supported on a sub-block. The test statistic of sLED links naturally to the fruitful results in Sparse Princi-

ple Component Analysis (SPCA), which is widely used for unsupervised dimension reduction in the high-dimensional regime. When testing covariance matrices, both theoretical and simulation results verify that sLED maintains the targeted size and is more powerful than many existing methods. We also illustrate that sLED can easily be generalized to comparisons between other relationship matrices, for example, the weighted adjacency matrices that are commonly used in gene clustering studies [Zhang and Horvath (2005)]. Applying sLED to the CMC data sheds lights on novel SCZ risk genes, and reveals intriguing patterns that are previously missed by the mean-based differential expression analysis.

The rest of this paper is organized as follows. In Section 2, we propose sLED for testing two-sample covariance matrices. We provide two algorithms to compute the test statistic, and establish theoretical guarantees on the consistency of sLED. In Section 3, we apply sLED to the CMC data. We detect a few hundred potential SCZ risk genes and reveal interesting patterns of gene co-expression changes. We also illustrate that sLED can be generalized to comparing other gene-gene relationship matrices, and we show the results of using weighted adjacency matrices. In Section 4, we conduct simulation studies and show that sLED outperforms many other existing two-sample covariance tests. Section 5 concludes the paper. All proofs are deferred to Appendix A and Appendix B.

## 2. Methods.

2.1. *Background.* Suppose RNA-sequencing is conducted on  $p$  genes for  $n$  case samples  $X_1, \dots, X_n \stackrel{i.i.d.}{\sim} (\mathbf{0}_p, \Sigma_1)$  and  $m$  control samples  $Y_1, \dots, Y_m \stackrel{i.i.d.}{\sim} (\mathbf{0}_p, \Sigma_2)$ , where  $X_i, Y_j \in \mathbb{R}^p$  independently come from two populations with potentially different covariance matrices. Without loss of generality, both expectations are assumed to be zero. Our goal is to test whether  $\Sigma_1 = \Sigma_2$ . Equivalently, let  $D = \Sigma_2 - \Sigma_1$  be the differential matrix, we want to test

$$H_0 : D = 0 \text{ versus } H_1 : D \neq 0. \quad (2.1)$$

This two-sample covariance testing problem has been well studied in the traditional large  $n$  small  $p$  setting, where the likelihood ratio test (LRT) is commonly used. However, testing covariance matrices under the high-dimensional regime is a nontrivial problem. In particular, the conventional LRT is no longer well defined when  $p > \min\{n, m\}$ . Even if  $p \leq \min\{n, m\}$ , Bai et al. (2009) shows that LRT performs poorly when  $p/\min\{n, m\} \rightarrow c \in (0, 1)$ .

There are several research lines that have proposed different methods to overcome this issue. The first line starts from rewriting (2.1) as

$$H_0 : \|D\|_F^2 = 0 \text{ versus } H_1 : \|D\|_F^2 \neq 0, \quad (2.2)$$

where  $\|D\|_F$  is the Frobenius norm of  $D$ . Then different estimators of  $\|D\|_F^2$  are used to form the test statistic. This line includes Schott (2007); Srivastava and Yanagihara (2010) under multivariate normality assumptions, and Li and Chen (2012) under more general settings. Such  $L_2$ -norm based tests are powerful when  $D$  is dense, but usually suffer from loss of power when the two covariance matrices

only differ at a small set of entries. On the other hand, [Cai, Liu and Xia \(2013\)](#) considers the sparse alternative where  $D$  has only a few non-zero elements. After forming [\(2.1\)](#) as

$$H_0 : \max_{1 \leq i, j \leq p} |D_{ij}| = 0 \text{ versus } H_1 : \max_{1 \leq i, j \leq p} |D_{ij}| \neq 0, \quad (2.3)$$

their test statistic is based on the estimation of  $\max_{i,j} |D_{ij}|$  after proper scaling. Later, [Chang, Zhou and Zhou \(2015\)](#) uses the same test statistic in a wild bootstrap procedure. These  $L_\infty$ -norm based tests have been shown to enjoy full power when the single-entry signal is strong, in the sense that the  $\max_{i,j} |D_{ij}|$  is at least on the order of  $\sqrt{\log p / \min\{n, m\}}$ .

In this paper, we focus on the unexplored but practically interesting regime where the signal is both sparse and weak, meaning that the difference may only occur at a small set of entries, while every difference tends to be small. We propose another perspective to construct the test statistic by looking at the singular value of  $D$ , which is especially suitable for this purpose. To illustrate the idea, consider a toy example where

$$D_{ij} = \begin{cases} \delta, & 1 \leq i, j \leq s \\ 0, & \text{otherwise} \end{cases} \quad (2.4)$$

for some  $\delta > 0$  and integer  $s \ll p$ . In other words,  $\Sigma_2$  and  $\Sigma_1$  are only different by  $\delta$  in an  $s \times s$  sub-block. In this case, the  $L_2$ -type tests are sub-optimal since they include noises from all entries, so are the  $L_\infty$ -type tests since they only utilize one single entry  $\delta$ . On the other hand, the largest singular value of  $D$  is  $s\delta$ , which extracts stronger signal with much less noise and therefore has the potential to gain more power.

More formally, we re-write the testing problem [\(2.1\)](#) to be the following equivalent form:

$$H_0 : \sigma_1(D) = 0 \text{ versus } H_1 : \sigma_1(D) \neq 0, \quad (2.5)$$

where  $\sigma_1(\cdot)$  denotes the largest singular value. Compared to [\(2.2\)](#) and [\(2.3\)](#), [\(2.5\)](#) provides a novel perspective to study the two-sample covariance testing problem based on the spectrum of the differential matrix  $D$ , and will be the starting point of constructing our test statistic.

*Notations.* We introduce the following notations for the rest of this paper. For a vector  $v \in \mathbb{R}^p$ ,  $\|v\|_q = (\sum_{i=1}^p |v_i|^q)^{1/q}$  denotes the usual  $L_q$  norm for  $q > 0$ , and let  $\|v\|_0$  represent the number of non-zero elements. For a symmetric matrix  $A \in \mathbb{R}^{p \times p}$ ,  $\|A\|_q$  denotes the  $L_q$  norm of vectorized  $A$ , and  $\text{tr}(A)$  denotes the trace. In addition,  $\lambda_1(A) \geq \dots \geq \lambda_p(A)$  represent the eigenvalues of  $A$ . Finally, for two symmetric matrices  $A, B \in \mathbb{R}^{p \times p}$ , we write  $A \succeq B$  when  $A - B$  is positive semidefinite.

*2.2. A two-sample covariance test: sLED.* After translating the testing problem to [\(2.5\)](#), we note that

$$\sigma_1(D) = \max\{|\lambda_1(D)|, |\lambda_1(-D)|\}.$$

Therefore, a naive test statistic would be  $T^{\text{naive}} = \max \left\{ \left| \lambda_1(\hat{D}) \right|, \left| \lambda_1(-\hat{D}) \right| \right\}$  for some estimator  $\hat{D}$ . A simple estimator is the difference between sample covariance matrices:

$$\hat{D} = \hat{\Sigma}_2 - \hat{\Sigma}_1, \text{ where } \hat{\Sigma}_1 = \frac{1}{n} \sum_{k=1}^n X_k X_k^T, \hat{\Sigma}_2 = \frac{1}{m} \sum_{l=1}^m Y_l Y_l^T. \quad (2.6)$$

However, in the high-dimensional setting,  $\lambda_1(\hat{D})$  is not necessarily a consistent estimator of  $\lambda_1(D)$ , and without extra assumptions, there is almost no hope of reliable recovery of the eigenvectors [Johnstone and Lu (2009)]. A popular remedy for such curse of dimensionality in many high-dimensional methods is to add sparsity assumptions, such as imposing an  $L_0$  constraint on an optimization procedure. Note that for any symmetric matrix  $A \in \mathbb{R}^{p \times p}$ ,

$$\lambda_1(A) = \max_{\|v\|_2=1} v^T A v = \max_{\|v\|_2=1} \text{tr}(A(vv^T)).$$

Now we can follow the common strategy to consider the following problem:

$$\lambda_1^R(A) = \max_{\|v\|_2=1, \|v\|_0 \leq R} \text{tr}(A(vv^T)), \quad (2.7)$$

where  $R > 0$  is some constant that controls the sparsity of the solution, and  $\lambda_1^R(A)$  is usually referred to as the  $R$ -sparse leading eigenvalue. Then, naturally, we construct the following test statistic

$$T_R = \max \left\{ \left| \lambda_1^R(\hat{D}) \right|, \left| \lambda_1^R(-\hat{D}) \right| \right\}, \quad (2.8)$$

and our sparse-Leading-Eigenvalue-Driven (sLED) test is obtained by thresholding  $T_R$  at the proper level.

Problem (2.7) is closely related with Sparse Principle Component Analysis (SPCA). The only difference is that in SPCA, the input matrix  $A$  is usually the sample covariance matrix, but here, we input the differential matrix  $\hat{D}$ . Solving (2.7) directly is computationally intractable, but we will show in Section 2.3 that it can be approximated using standard SPCA approaches.

Finally, since it is difficult to obtain the limiting distribution of  $T_R$ , we use a permutation procedure. Specifically, for any  $\alpha \in (0, 1)$ , the  $\alpha$ -level sLED, denoted by  $\Psi_\alpha$ , is obtained as follows:

1. Given samples  $Z = (X_1, \dots, X_n, Y_1, \dots, Y_m)$ , calculate the test statistic  $T_R$  as in (2.8).
2. Sample uniformly from  $Z$  without replacement to get  $Z^* = (Z_1^*, \dots, Z_N^*)$ , where  $N = n + m$ .
3. Calculate the permutation differential matrix  $\hat{D}^*$ :

$$\hat{D}^* = \hat{\Sigma}_2^* - \hat{\Sigma}_1^*, \quad (2.9)$$

where  $\hat{\Sigma}_1^* = \frac{1}{n} \sum_{k=1}^n Z_k^* (Z_k^*)^T$ ,  $\hat{\Sigma}_2^* = \frac{1}{m} \sum_{l=n+1}^N Z_l^* (Z_l^*)^T$ .

4. Obtain the permutation test statistic

$$T_R^* = \max \left\{ \left| \lambda_1^R(\hat{D}^*) \right|, \left| \lambda_1^R(-\hat{D}^*) \right| \right\}. \quad (2.10)$$

5. Repeat steps 2 – 4 for  $B$  times to get  $T_R^{*(1)}, \dots, T_R^{*(B)}$ , then estimate the  $p$ -value

$$\hat{p} = \frac{1}{B} \sum_{b=1}^B I_{\{T_R^{*(b)} > T_R\}},$$

and sLED rejects  $H_0$  if  $\hat{p} < \alpha$ , i.e.,  $\Psi_\alpha = I_{\{\hat{p} < \alpha\}}$ .

*Remark.* We can also estimate the support of the  $R$ -sparse leading eigenvector of  $D$ , which provides a list of potential risk genes. Without loss of generality, suppose  $\lambda_1^R(\hat{D}) > \lambda_1^R(-\hat{D})$ , we define

$$\text{Leverage} := \text{diag}(\hat{v}\hat{v}^T) = (\hat{v}_1^2, \dots, \hat{v}_p^2)^T, \quad (2.11)$$

where  $\hat{v}$  is the  $R$ -sparse leading eigenvector of  $\hat{D}$  in (2.7). Then the elements with large leverage will be the candidate genes that have altered covariance structure between the two populations.

*2.3. Sparse principle component analysis.* There are many studies on Sparse Principle Component Analysis (SPCA) that provide various algorithms to approximate (2.7) when  $A$  is a sample covariance matrix. Most techniques utilize an  $L_1$  constraint to achieve both sparsity and computational efficiency. To name a few, [Jolliffe, Trendafilov and Uddin \(2003\)](#) forms the SCoTLASS problem by directly replacing the  $L_0$  constraint by  $L_1$  constraint, and uses a projected gradient descent algorithm. Later on, [Zou, Hastie and Tibshirani \(2006\)](#) analyzes the problem from a penalized regression perspective, and [Witten, Tibshirani and Hastie \(2009\)](#); [Shen and Huang \(2008\)](#) start from the low rank matrix completion and approximation framework. In addition, there is another line of studies that considers convex relaxations of (2.7), including the SDP relaxation in [d'Aspremont et al. \(2007\)](#) and the convex hull relaxation using Fantope in [Vu et al. \(2013\)](#).

For the purpose of this paper, we only give details of the following two methods that can be directly generalized to approximates (2.7) with input matrix being  $\hat{D}$ , the differential matrix.

*Fantope projection and selection (FPS).* For a symmetric matrix  $A \in \mathbb{R}^{p \times p}$ , FPS [[Vu et al. \(2013\)](#)] considers a convex optimization problem:

$$\lambda_{fps}^R(A) = \max_{H \in \mathcal{F}^1, \|H\|_1 \leq R} \text{tr}(AH), \quad (2.12)$$

where  $\mathcal{F}^1 = \{H \in \mathbb{R}^{p \times p} : \text{symmetric}, 0 \preceq H \preceq I, \text{tr}(H) = 1\}$  is the 1-dimensional Fantope, which is the convex hull of 1-dimensional projection matrices  $\{vv^T : \|v\|_2 = 1\}$ . In addition, by Cauchy-Schwarz inequality, if  $\|v\|_2 = 1$ , then  $\|vv^T\|_1 \leq \|v\|_0$ . Therefore, (2.12) is a convex relaxation of (2.7). Moreover, when the input matrix is  $\hat{D}$ , the problem is still convex, and the ADMM algorithm proposed in [Vu](#)

et al. (2013) can be directly applied. This algorithm has guaranteed convergence, but requires iteratively performing SVD on a  $p \times p$  matrix. This calculation further needs to be repeated  $B$  times in the permutation testing procedure, and becomes computationally demanding when  $p$  is on the order of a few thousands. Therefore, we present an alternative heuristic algorithm below, which is much more efficient and typically works well in practice.

*Penalized matrix decomposition (PMD).* For a general matrix  $A \in \mathbb{R}^{p \times p}$ , PMD [Witten, Tibshirani and Hastie (2009)] solves a rank-1 matrix completion problem:

$$\lambda_{pmd}^R(A) = \max_{u,v} \text{tr} (A (uv^T)) , \tag{2.13}$$

subject to  $\|u\|_2 \leq 1, \|v\|_2 \leq 1, \|u\|_1 \leq \sqrt{R}, \|v\|_1 \leq \sqrt{R}$ .

The solution for each one of  $u$  and  $v$  has a simple closed form after fixing the other one. This gives a straightforward iterative algorithm, and is implemented in the R package PMA. If the solutions further satisfy  $\hat{u} = \hat{v}$ , then they are also the solutions to the following non-convex Constrained-PMD problem:

$$\lambda_{c-pmd}^R(A) = \max_{\|v\|_2 \leq 1, \|v\|_1 \leq \sqrt{R}} \text{tr} (A (vv^T)) . \tag{2.14}$$

Note that the solutions of (2.14) always have  $\|v\|_2 = 1$ , which implies  $\|v\|_1^2 = \|vv^T\|_1 \leq \|v\|_0$ , so (2.14) is also an approximation to (2.7). Now observe that when  $A \succeq 0$ , as in the usual SPCA setting, the solutions of (2.13) automatically have  $\hat{u} = \hat{v}$  by Cauchy-Schwarz inequality. However, this is no longer true when  $A$  is not positive semidefinite, as when we deal with the differential matrix  $\hat{D}$ . To overcome this, we choose some constant  $d > 0$  that is large enough such that  $A + dI \succeq 0$ . Then the solutions of  $\lambda_{pmd}^R(A + dI)$  will satisfy  $\hat{u} = \hat{v}$ , and it is easy to obtain  $\lambda_{c-pmd}^R(A)$  by

$$\lambda_{c-pmd}^R(A) = \lambda_{pmd}^R(A + dI) - d . \tag{2.15}$$

*2.4. Consistency.* Finally, we show that sLED is consistent when testing covariance matrices. The validity of its size is guaranteed by permutation procedure. Here, we prove that sLED also achieves full power asymptotically, under the following assumptions:

- (A1) (Balanced sample sizes)  $\underline{c}n \leq m \leq \bar{c}n$  for some constants  $0 < \underline{c} \leq 1 \leq \bar{c} < \infty$ .
- (A2) (Sub-gaussian tail) Let  $(Z_1, \dots, Z_N) = (X_1, \dots, X_n, Y_1, \dots, Y_m)$ , then every  $Z_k$  is sub-gaussian with parameter  $\nu^2$ , that is,

$$\mathbb{E} \left[ e^{t(Z_k^T u)} \right] \leq e^{\frac{t^2 \nu^2}{2}}, \quad \forall t > 0, \forall u \in \mathbb{R}^p \text{ such that } \|u\|_2 = 1 .$$

- (A3) (Dimensionality)  $(\log p)^3 \leq O(n)$ .
- (A4) (Signal strength) Under  $H_1$ , for some constant  $C$  to be specified later,

$$\max \{ \lambda_1^R(D), \lambda_1^R(-D) \} \geq CR \sqrt{\frac{\log p}{n}} .$$

**THEOREM 1 (Power of sLED).** *Let  $T_R$  be the test statistic as defined in (2.8), and  $T_R^*$  be the permutation test statistic as defined in (2.10), where  $\lambda_1^R(\cdot)$  is approximated by  $L_1$ -constrained algorithms (2.12) or (2.14). Then under assumptions (A1)-(A3), for  $\forall \delta > 0$ , there exists a constant  $C$  depending on  $(\underline{c}, \bar{c}, \nu^2, \delta)$ , such that if assumption (A4) holds, after  $(n, p)$  being large enough,*

$$\mathbb{P}_{H_1} \left( T_R(\hat{D}^*) > T_R(\hat{D}) \right) \leq \delta.$$

*As a consequence, for any pre-specified level  $\alpha \in (0, 1)$ , pick  $\delta = \frac{\alpha}{2}$ , then*

$$\mathbb{P}_{H_1} (\Psi_\alpha = 1) \rightarrow 1 \text{ as } B \rightarrow +\infty.$$

The proof of theorem 1 contains two main steps. First, theorem 2 provides an upper bound of the entries in  $\hat{D}^*$ . After then, theorem 3 ensures that the permutation test statistic  $T_R^*$  is controlled by  $\|\hat{D}^*\|_\infty$ , and the test statistic  $T_R$  is lower-bounded in terms of the signal strength. The proof details are presented in Appendix A.

**THEOREM 2 (Permutation differential matrix).** *Under assumptions (A1)-(A3), let  $\hat{D}^*$  be the permutation differential matrix as defined in (2.9), then  $\forall \delta > 0$ , there exist constants  $C, C_1$  depending on  $(\nu^2, \underline{c}, \bar{c})$ , such that after  $(n, p)$  being large enough,*

$$\mathbb{P} \left( \|\hat{D}^*\|_\infty > C \sqrt{\frac{\log(C_1 p^2 / \delta)}{n}} \right) \leq \delta.$$

**THEOREM 3 (Test statistic).** *For any symmetric matrix  $\hat{D}$ , let  $\tilde{\lambda}_1^R(\hat{D})$  be a solution of the  $L_1$ -constrained algorithms (2.12) or (2.14), then the following statements hold:*

- (i) *If  $\|\hat{D}\|_\infty \leq \delta$ , then  $\tilde{\lambda}_1^R(\hat{D}) \leq R\delta$ .*
- (ii) *If there is a matrix  $D$  such that  $\|\hat{D} - D\|_\infty \leq \delta$ , then*

$$\tilde{\lambda}_1^R(\hat{D}) \geq \lambda_1^R(D) - R\delta.$$

*Remark 1.* Assumption (A4) does not assume the leading eigenvector of  $D$  (or  $-D$ ) to be sparse. It only needs the sparse signal to be strong enough, which is a very mild requirement. In addition, the required sparse signal level,  $O\left(R\sqrt{\log p/n}\right)$ , matches the rate in Berthet and Rigollet (2013), where it is shown to be the optimal detection rate for any polynomial-time algorithm.

In fact, Berthet and Rigollet (2013) also shows that without the computational constraint, the optimal signal strength is on the order of  $\sqrt{R \log / n}$ . Here, we show that this rate can also be achieved by sLED if we use the exact solutions of the  $L_0$ -constrained problem (2.7). For this purpose, we introduce two slightly different assumptions as follows:

$$(A3') \text{ (Dimensionality) } R = o(p), \quad R^5(\log p)^3 \leq O(n).$$

(A4') (Signal strength) Under  $H_1$ , for some constant  $C$  to be specified later,

$$\max \{ \lambda_1^R(D), \lambda_1^R(-D) \} \geq C \sqrt{\frac{R \log p}{n}}.$$

Now we state the results regarding the  $L_0$ -constrained solutions, and detailed proofs are shown in Appendix B.

**THEOREM 4** (Power of sLED without computational constraint). *Let  $T_R$  be the test statistic as defined in (2.8) where  $\lambda_1^R(\cdot)$  is the global optimum of (2.7). Then under assumptions (A1)-(A2) and (A3'), for any pre-specified level  $\alpha \in (0, 1)$ , there exists a constant  $C$  depending on  $(\underline{c}, \bar{c}, \nu^2, \alpha)$ , such that if assumption (A4') holds, after  $(n, p)$  being large enough,*

$$\mathbb{P}_{H_1}(\Psi_\alpha = 1) \rightarrow 1 \text{ as } B \rightarrow +\infty.$$

*Remark 2.* Recall the toy example in (2.4). If we let  $R = s$ , then the  $R$ -sparse leading eigenvalue of  $D$  is  $\lambda_1^R(D) = s\delta$ , and sLED remains powerful for  $\delta$  as small as  $\sqrt{\log p / (ns)}$ . On the other hand, the maximal entry method in Cai, Liu and Xia (2013) cannot succeed under this setting since it requires  $\delta$  to be at least on the order of  $\sqrt{\log p / n}$  or higher.

**2.5. Choosing sparsity parameter  $R$ .** The tuning parameter  $R$  plays an important role in the sLED test. If  $R$  is too large, the method uses little regularization and assumption (A4) is unlikely to hold. If  $R$  is too small, then the constraint is too strong to uncover the signal in the differential matrix. In practice, sLED requires an appropriate choice of  $R$ . We know that  $R$  provides a natural, but possibly loose, lower bound on the support size of the estimated sparse eigenvector. In general, one can use cross-validation to choose  $R$ , so that the estimated leading sparse singular vector maximizes its inner product with a differential matrix computed from a testing subsample.

Theoretically one can show that  $R$  provides a lower bound on the number of selected genes. In applications, one can often choose  $R$  with the aid of subject background knowledge. For example, in the study of the co-expression of genes in Schizophrenia patients versus controls, we target, at most, a certain proportion of the genes for further investigation. One can use this upper bound to select  $R$  to match the desired number of potential discoveries.

**3. Application to Schizophrenia data.** In this section, we apply sLED to the CommonMind Consortium (CMC) data, with RNA-sequencing on 16,423 genes from 258 Schizophrenia (SCZ) subjects and 279 control samples [Fromer et al. (2016)]. The raw data are log-transformed and various clinical covariates are regressed out, including age, gender, site, batch, post-mortem interval (PMI), and RNA integrity number (RIN). We also center and standardize the expression data so that each gene has mean 0 and standard deviation 1. Therefore, the covariance test is applied to correlation matrices.

3.1. *Preprocess: gene modules.* To reduce the computational burden and enhance interpretability of the results, we first cluster the 16,423 genes into different modules, such that genes within each module are densely interconnected, which could be a result of closely related biological functions. This approach has been widely adopted in the literature, and one popular approach is WGCNA [Zhang and Horvath (2005)], which has been shown to yield biologically reasonable gene modules. WGCNA uses a weighted adjacency matrix  $A \in \mathbb{R}^{p \times p}$ , calculated as

$$A_{ij} = |R_{ij}|^\beta, \text{ for } 1 \leq i, j \leq p \text{ and } \beta > 0, \quad (3.1)$$

where  $R_{ij}$  is the Pearson correlation between gene  $i$  and gene  $j$ . The power  $\beta > 0$  is a parameter that essentially controls the average node “degrees” in the weighted network. Here we construct the weighted adjacency matrix based on 279 control samples with  $\beta = 6.5$  as in Fromer et al. (2016). To minimize the effects of noise, the adjacency matrix  $A$  is further transformed into a Topological Overlap Matrix (TOM) [Ravasz et al. (2002)], from which a hierarchical clustering tree is obtained. Finally, after a dynamic tree cut, a total of 12,834 genes are assigned into 35 genetic modules, each containing at least 30 genes and labeled by a color. The remaining 3,589 genes are un-clustered and colored as *grey*, and are removed from the following analysis (Figure 1).

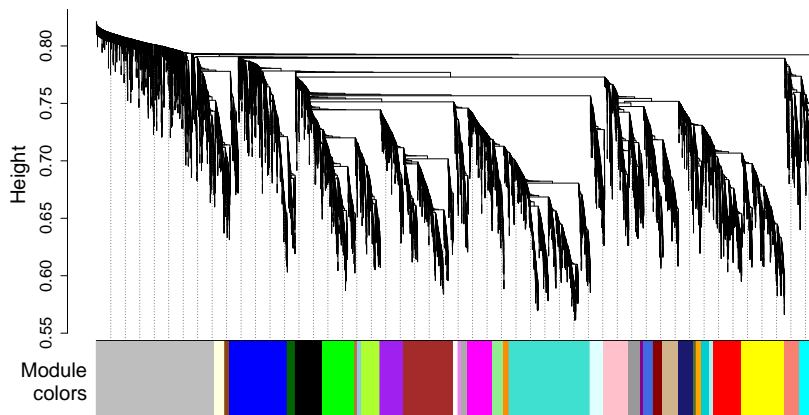


FIG. 1. 35 Modules clustered by WGCNA, each labeled by a color. The first grey block contains 3,589 un-clustered genes.

3.2. *Testing covariance matrices.* We apply sLED to the 35 modules separately, each with 1,000 permutation repetitions. Following Witten, Tibshirani and Hastie (2009), we solve the sparse eigenvalue problem (2.14) for  $\sqrt{R} = c\sqrt{p}$  some  $c \in (0, 1)$ , such that the estimated sparse eigenvector  $\hat{v}$  has the desired level of sparsity. Here, since the number of key genes that carry the genetic signals is expected to be roughly in the range of 1%–10%, and we know that  $c^2$  provides a loose lower bound

on the proportion of discovered genes, we choose  $c = 0.1$  for all modules that have at least 100 genes. For the 12 modules containing less than 100 genes, due to the implicit requirement of  $c\sqrt{p} \geq 1$  in (2.14), we use  $c = 0.2$  instead. Finally, we apply the Benjamini-Hochberg procedure to control the false-discovery-rate (FDR) at 0.2 across 35 modules [Benjamini and Hochberg (1995)]. The cut-off occurs at the 4-th smallest  $p$ -value, 0.017, and hence the first 4 modules are significant (Figure 2). These include the *blue* and *yellow* modules that are also reported by Fromer et al. (2016).

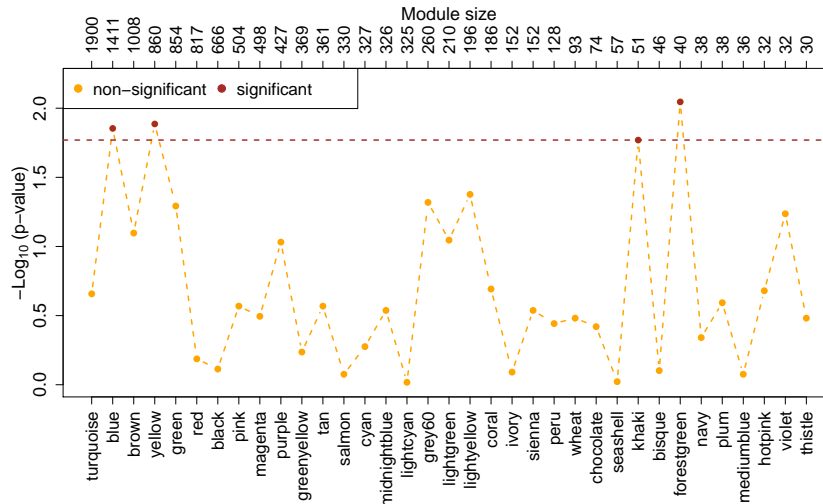


FIG. 2.  $P$ -values of  $sLED$  on 35 modules, each with 1000 permutation repetitions, plotted in the  $-\log_{10}(\cdot)$  scale. Modules are ordered by their sizes in descending order. The horizontal line shows the cut-off at 0.017, obtained by the Benjamini-Hochberg procedure of false-discovery-rate control at 0.2.

We then identify key genes in the significant modules according to their leverage, as defined in (2.11). Specifically, we first order the leverage such that  $\hat{v}_{(1)}^2 \geq \hat{v}_{(2)}^2 \geq \dots \geq \hat{v}_{(p)}^2$ . Because  $\sum_{i=1}^p \hat{v}_{(i)}^2 = 1$ , we can use a scree plot to find the top few genes that contribute the most to the total leverage. We choose the first  $q$  genes such that  $\sum_{i=1}^q \hat{v}_{(i)}^2 \geq 0.999$ , which we call primary genes. The remaining genes with non-zero leverage are referred to as secondary genes, which account for the remaining 0.001 leverage (see Figure 3a for an example). The annotated names of 45 primary genes identified in this way from 4 significant modules are listed in Table 1. Among these, only 5 genes show differential expression from Fromer et al. (2016) analyses.

Next, we take a closer look at the largest significant module, the *blue* module, whose  $p$ -value is 0.014. There are 105 top genes that have non-zero leverage, and the first 25 primary genes achieve a total leverage of 0.999. We show in Figure 3b how these 105 top genes form a clear block structure in the differential matrix  $\hat{D} = \hat{\Sigma}_{control} - \hat{\Sigma}_{SCZ}$ . Notably, such a block structure cannot be revealed if ordered by the differentially expressed  $p$ -values (Figure 3c).

TABLE 1  
 45 primary genes detected in 4 significant modules, listed by the descending order of leverage.  
 The 5 underlined genes are also detected by differential expression analysis

Module	Primary gene names
blue	ABHD2, SLC23A2, LRRC55, KCTD10, ZBTB24, CRKL, TUBGCP3, WBP11, REXO2, USP13, <u>FNIP2</u> , MORC2-AS1, OSBP, SNX30, TGOLN2, HEXIM1, <u>TOX3</u> , SYT11, HNMT, ISCA2, SMAD3, PURB
yellow	ARSB, PRUNE2, <u>SESTD1</u> , BCOR, USP30, BACE1, ZKSCAN1, DNAJB7, <u>TAOK1</u> , CBWD5, TTC3-AS1, TATDN2P2, TTLL7-IT1, ZNF10, FOXP3, FBXO32, SPPL3
khaki	QRICH1, <u>TCTA</u> , ADIPOR1, GLB1
forestgreen	NDUFB11, MIR31HG

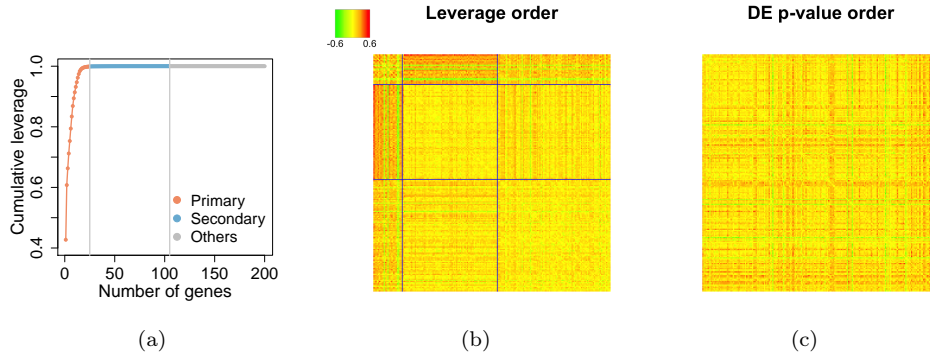


FIG. 3. Selected 200 genes in blue module, including 25 primary genes that account for a total leverage of 0.999, 80 secondary genes that account for the remaining 0.001 leverage, and 95 randomly selected other genes that have zero leverage. (a) Scree plot of cumulative leverage. (b) Heatmap of  $\hat{D}$  where genes are ordered by leverage and a block structure is revealed. The two partitioning lines indicate the 25 primary genes and the 80 secondary genes. (c) Heatmap of  $\hat{D}$  where genes are ordered by p-values in differential expression analysis. Now the block structure is diluted.

Figure 3b reveals a significant decrease of gene co-expression (interactions) in cortical samples from SCZ subjects between the 25 primary genes and the 80 secondary genes. This pattern is more clearly illustrated in Figure 4, where two gene networks are constructed for these 105 genes in control samples and SCZ samples separately (see Table 2 for gene names).

To shed light on the nature of the genes identified in the blue module, we conduct a Gene Ontology (GO) enrichment analysis [Chen et al. (2013)]. The secondary gene list is most easily interpreted. It is highly enriched for genes directly involved in synaptic processes, both for GO Biological Process and Molecular Function. Two key molecular functions involve calcium channels/calcium ion transport and glutamate receptor activity. Under Biological Process, these themes are emphasized and synaptic organization emerges too. Synaptic function is a key feature that emerges from genetic findings for SCZ, including calcium channels/calcium ion transport

and glutamate receptor activity [see [Owen, Sawa and Mortensen \(2016\)](#) for review].

For the primary genes, under GO Biological Process, “*regulation of transforming growth factor beta2 (TGF-β2) production*” is highly enriched. The top GO Molecular Function term is SMAD binding. The protein product of SMAD3 (one of the primary genes) modulates the impact of transcription factor TGF-β regarding its regulation of expression of a wide set of genes. TGF-β is important for many developmental processes, including the development and function of synapses [[Diniz et al. \(2012\)](#)]. Moreover, and notably, it has recently been shown that SMAD3 plays a crucial role in synaptogenesis and synaptic function via its modulation of how TGF-β regulates gene expression [[Yu et al. \(2014\)](#)]. It is possible that disturbed TGF-β signaling could explain co-expression patterns we observe in Figure 4, because this transcription factor will impact multiple genes. On the other hand, within the set of primary genes, another gene of interest is OSBP. Its protein product has recently been shown to regulate neural outgrowth and thus synaptic development [[Gu et al. \(2015\)](#)]. Thus perturbation of a set of genes could explain the pattern seen in Figure 4.

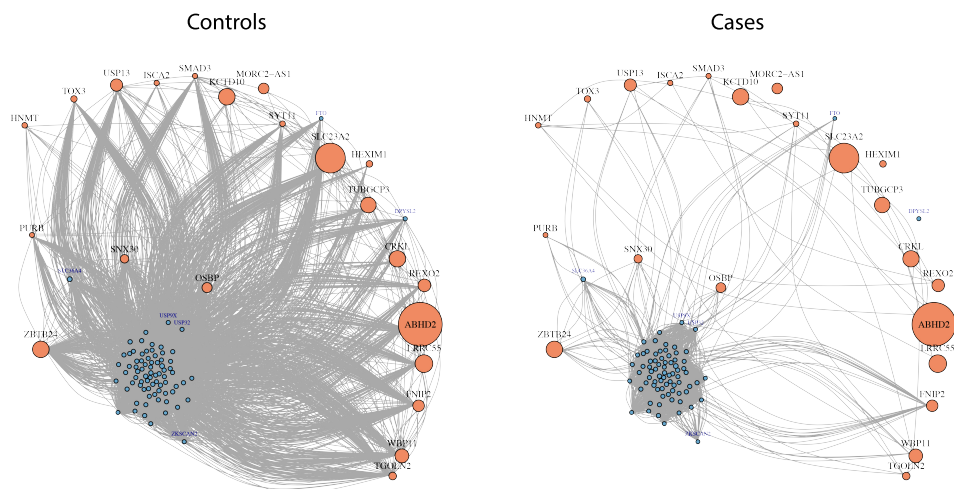


FIG. 4. Gene networks constructed from control and SCZ samples, using top genes in blue module that have non-zero leverage. We exclude 6 genes that do not have annotated gene names, and show the remaining 22 primary genes (colored as orange) and 77 secondary genes (colored as blue). The adjacency matrix is constructed by thresholding the absolute Pearson correlation  $|R_{ij}|$  at 0.5. Larger node sizes represent larger leverage.

3.3. *Testing weighted adjacency matrices.* Finally, we illustrate that sLED is not only applicable to testing differences in covariance matrices, but also to the comparisons between two general “relationship” matrices, including the weighted adjacency matrix  $A$  as defined in (3.1). Specifically, we consider  $D = \mathbb{E}(A_{control}) - \mathbb{E}(A_{SCZ})$ , and the testing problem

$$H_0 : D = 0 \text{ versus } H_1 : D \neq 0.$$

TABLE 2  
Annotated names of 22 primary genes and 77 secondary genes in blue module, listed in the descending order of leverage. The 6 underlined genes are also significant in the differential expression analysis

Gene names	
Primary genes	ABHD2 SLC23A2 LRRC55 KCTD10 ZBTB24 CRKL TUBGCP3 WBP11 REXO2 USP13 <u>FNIP2</u> MORC2-AS1 OSBP SNX30 TGOLN2 HEXIM1 <u>TOX3</u> SYT11 HNMT ISCA2 SMAD3 PURB
Secondary genes	SLC36A4 HECW2 STOX2 C1orf173 DLG2 ITSN1 PPM1L <u>DNM3</u> LRRTM3 LRRTM4 DPYSL2 ANK2 ANK3 EIF4G3 PUM1 SYNPO2 NTNG1 DNAJC6 SLIT2 OPRM1 RASAL2 ATP8A2 CKAP5 CNTNAP2 GNPTAB PPP1R12B CAMTA1 SATB1 ANKRD17 THRB NIPAL2 MAP1B STAM RYR2 TRPC5 ST8SIA3 SHROOM2 PTPRK USP9X ZKSCAN2 KIAA1549L KIAA1279 MYH10 USP32 ARHGAP32 SLITRK1 WHSC1L1 AKAP11 ARHGAP24 BTRC SLC24A2 JPH1 KIAA1244 TSC1 NOVA1 MFSD6 NRCAM <u>NLGN1</u> LMO7 ADAM23 RAPGEF2 KIAA1217 UNC80 GRIN2A <u>RASA1</u> <u>KCNJ6</u> GRM1 PCNX GRM7 PBX1 HECW1 CDKL5 MYO5A MYT1L HSPA12A DLGAP1 FTO

While classical two-sample covariance testing procedures are inapplicable under this setting, sLED can be easily generalized to incorporate this scenario. Let  $\hat{D} = A_{control} - A_{SCZ}$ , then the same permutation procedure as described in Section 2.2 can be applied, using the same SPCA algorithms.

Again, as an example, we illustrate the results on the *blue* module. We apply sLED with  $c = 0.1$  (i.e.,  $\sqrt{R} = 0.1\sqrt{p}$  in (2.14)) to the weighted adjacency matrices using  $\beta \in \{1, 3, 6.5, 9\}$ . With 1,000 permutations, the  $p$ -values are 0.024, 0.004, 0.006, and 0.002, respectively. The latter three are significant at level 0.05 after a Bonferroni correction. Interestingly, we find our results to be closely related to the connectivity of genes within a module, which is a generalized definition of node degree:

$$k_i = \sum_{j \neq i} A_{ij} \text{ for gene } i.$$

The connectivity of genes is typically higher in control samples; we highlight the top genes with non-zero leverage in sLED in Figure 5. We can see that as  $\beta$  increases, the differences on highly connected genes are enlarged, and consistently, the top genes detected by sLED also concentrate more and more on these “hub” genes that are densely connected. These genes would have been missed by the covariance matrix test, but are now revealed after transforming to weighted adjacency matrices. A Gene Ontology (GO) enrichment analysis [Chen et al. (2013)] finds that the list of top genes detected when  $\beta = 9$  reveals more neuro-related biological processes than the top genes detected when  $\beta = 1$  (Table 3).

**4. Simulations.** Finally, we conduct simulation studies to compare the size and power of sLED with other existing methods, including Li and Chen (2012) that uses the Frobenius norm of  $D$  (Frob), Cai, Liu and Xia (2013) that uses the maximal absolute entry of  $D$  (Max), Chang, Zhou and Zhou (2015) that uses a wild

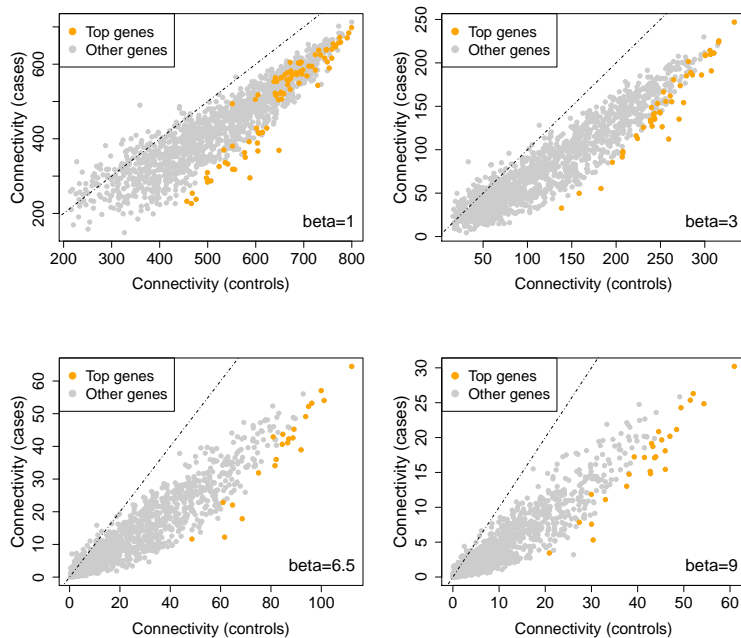


FIG. 5. Connectivity within blue module in control and SCZ samples using weighted adjacency matrices with different  $\beta$ . The top genes with non-zero leverage is highlighted in orange.

TABLE 3

Top 5 terms in Gene Ontology (GO) enrichment analysis on top genes with non-zero leverage, using weighted adjacency matrices with different  $\beta$

	Top 5 GO terms	P-value
$\beta = 1$	positive regulation of cell development (GO:0010720)	8.8e-05
	divalent metal ion transport (GO:0070838)	2.8e-05
	divalent inorganic cation transport (GO:0072511)	3.1e-05
	calcium ion transport (GO:0006816)	1.2e-04
	regulation of transporter activity (GO:0032409)	1.4e-04
$\beta = 9$	synaptic transmission (GO:0007268)	7.5e-06
	energy reserve metabolic process (GO:0006112)	8.0e-06
	divalent metal ion transport (GO:0070838)	5.1e-05
	divalent inorganic cation transport (GO:0072511)	5.5e-05
	calcium ion transport (GO:0006816)	3.4e-05

bootstrap on the same test statistic (**MaxBoot**), and [Wu and Li \(2015\)](#) that uses random matrix projections (**RandProj**).

We consider the following two types of differential matrix  $D = \Sigma_2 - \Sigma_1$ :

- (i) Spiked difference:  $D = \theta vv^T$ , with  $\|v\|_2 = 1$ ,  $\|v\|_0 = \lfloor p/10 \rfloor$ , and  $\theta = 3$ , where  $\lfloor x \rfloor$  denotes the largest integer that is smaller or equal to  $x$ . The support of  $v$  is uniformly sampled from the set  $\{1, \dots, p\}$  without replacement, and its elements are first sampled from  $N(1, 0.01)$  and then normalized to have unit  $L_2$  norm. Note that  $\theta$  does not grow with  $n$  and  $p$ , so the effective signal strength becomes smaller as  $p$  increases.
- (ii) Block difference:  $D_{ij} = \begin{cases} 0.1, & \lfloor p/10 \rfloor(k-1) + 1 \leq i \neq j \leq \lfloor p/10 \rfloor k, \\ & \text{for } k = 1, 2, 3; \\ 0, & \text{otherwise.} \end{cases}$

And for each choice of  $D$ , we explore three choices of  $\Sigma_1$ :

- (i) Identity matrix:  $\Sigma_1 = I_p$ .
- (ii) Block diagonal:  $\Sigma_{1,ij} = \begin{cases} 1, & i = j; \\ 0.5, & \lfloor p/10 \rfloor(k-1) + 1 \leq i \neq j \leq \lfloor p/10 \rfloor k, \\ & \text{for } k = 1, \dots, 10; \\ 0, & \text{otherwise.} \end{cases}$
- (iii) Bandable:  $\Sigma_{1,ij} = r^{|i-j|}$ , where  $r = 0.5$ .

With nominal level  $\alpha = 0.05$ , [Table 4](#) reports the actual sizes and powers under sample sizes  $n = m = 100$ , with  $p$  varying over  $\{100, 300, 500\}$ . For each model, samples are generated independently using multivariate Gaussian with mean zero. We always use  $\sqrt{R} = 0.3\sqrt{p}$  in [\(2.14\)](#) for **sLED**. We see that **sLED**, along with **Max**, **MaxBoot** and **RandProj**, have the best control over empirical size. In terms of power, **sLED** outperforms all other tests in most cases. Although **Frob** is sometimes more powerful, it also tends to be anti-conservative under  $H_0$ .

**5. Conclusion and discussion.** In this paper, we propose **sLED**, a permutation test for two-sample covariance matrices under the high dimensional regime, which meets the need to understand the changes of gene interactions in complex human diseases. We prove that **sLED** achieves asymptotically full power; and in many biologically plausible settings, we verify by simulation studies that **sLED** outperforms many other existing methods and maintains valid size in finite samples. We apply **sLED** to a recently produced gene expression data set on Schizophrenia, and provide a list of 45 genes that show altered co-expression when brain samples from cases are compared to that from controls. We also reveal an interesting pattern of gene correlation change that has not been previously detected. The biological basis for this pattern is unclear. As more gene expression data become available, it will be interesting to validate these findings in an independent data set.

We point out that the detection of top genes can have stronger theoretical guarantees under some extra sparsity assumptions on the differential matrix  $D$ . In fact, following the proofs in [Vu et al. \(2013\)](#); [Lei and Vu \(2015\)](#), an exact support re-

TABLE 4  
*Empirical sizes and powers with sample size  $n = m = 100$  and nominal level  $\alpha = 0.05$ . Each result is the average of 500 replications*

<b>D</b>	$\Sigma_1$ <b>p</b>	<b>Identity</b>			<b>Block diagonal</b>			<b>Bandable</b>		
		<b>100</b>	<b>300</b>	<b>500</b>	<b>100</b>	<b>300</b>	<b>500</b>	<b>100</b>	<b>300</b>	<b>500</b>
Empirical size										
–	sLED	0.05	0.05	0.05	0.05	0.03	0.05	0.05	0.04	0.04
	Frob	0.10	0.42	0.81	0.11	0.10	0.11	0.10	0.25	0.47
	Max	0.04	0.05	0.02	0.06	0.05	0.05	0.04	0.05	0.04
	MaxBoot	0.05	0.05	0.03	0.06	0.07	0.07	0.05	0.04	0.06
	RandProj	0.06	0.05	0.07	0.03	0.07	0.07	0.05	0.05	0.07
Empirical power										
Spiked	sLED	0.99	0.75	0.37	0.32	0.05	0.04	0.84	0.21	0.08
	Frob	0.75	0.69	0.89	0.22	0.11	0.10	0.47	0.38	0.54
	Max	0.13	0.05	0.02	0.15	0.05	0.04	0.18	0.06	0.05
	MaxBoot	0.18	0.08	0.08	0.17	0.06	0.06	0.14	0.06	0.05
	RandProj	0.14	0.09	0.08	0.13	0.07	0.06	0.10	0.07	0.06
Block	sLED	0.10	0.72	0.96	0.11	0.10	0.12	0.12	0.45	0.79
	Frob	0.31	0.96	1.00	0.14	0.13	0.16	0.20	0.63	0.94
	Max	0.04	0.06	0.06	0.06	0.04	0.04	0.05	0.06	0.06
	MaxBoot	0.06	0.07	0.06	0.06	0.05	0.06	0.08	0.05	0.07
	RandProj	0.06	0.09	0.07	0.06	0.06	0.06	0.07	0.06	0.07

covery of the principal subspace of  $D$  can be achieved. We omit these theoretical results since the required assumptions tend to be too stringent on the CMC data.

Finally, we illustrate that sLED can be applied to a more general class of differential matrices. We show an example of comparing two weighted adjacency matrices and how this reveals novel insight on Schizophrenia. This is a first step towards testing general high-dimensional matrices, and we leave a more thorough exploration in this direction to future work.

**Acknowledgements.** This work was supported by the Simons Foundation (SFARI 124827), National Institute of Mental Health grant R37MH057881 (Bernie Devlin and Kathryn Roeder) and National Science Foundation DMS-1407771 (Jing Lei).

## References.

- ANDERSON, T. W., ANDERSON, T. W., ANDERSON, T. W. and ANDERSON, T. W. (1958). *An introduction to multivariate statistical analysis* **2**. Wiley New York.
- BAI, Z., JIANG, D., YAO, J.-F. and ZHENG, S. (2009). Corrections to LRT on large-dimensional covariance matrix by RMT. *The Annals of Statistics* 3822–3840.
- BARDENET, R., MAILLARD, O.-A. et al. (2015). Concentration inequalities for sampling without replacement. *Bernoulli* **21** 1361–1385.
- BENJAMINI, Y. and HOCHBERG, Y. (1995). Controlling the false discovery rate: a practical and powerful approach to multiple testing. *Journal of the Royal Statistical Society. Series B (Methodological)* 289–300.
- BERTHET, Q. and RIGOLLET, P. (2013). Optimal detection of sparse principal components in high dimension. *The Annals of Statistics* **41** 1780–1815.
- CAI, T., LIU, W. and XIA, Y. (2013). Two-sample covariance matrix testing and support recovery in high-dimensional and sparse settings. *Journal of the American Statistical Association* **108** 265–277.
- CHANG, J., ZHOU, W. and ZHOU, W.-X. (2015). Bootstrap Tests on High Dimensional Covariance Matrices with Applications to Understanding Gene Clustering. *arXiv preprint arXiv:1505.04493*.
- CHEN, E. Y., TAN, C. M., KOU, Y., DUAN, Q., WANG, Z., MEIRELLES, G. V., CLARK, N. R. and MA'AYAN, A. (2013). Enrichr: interactive and collaborative HTML5 gene list enrichment analysis tool. *BMC Bioinformatics* **14** 128.
- INTERNATIONAL SCHIZOPHRENIA CONSORTIUM, PURCELL, S. M., WRAY, N. R., STONE, J. L., VISSCHER, P. M., O'DONOVAN, M. C., SULLIVAN, P. F. and SKLAR, P. (2009). Common polygenic variation contributes to risk of schizophrenia and bipolar disorder. *Nature* **460** 748–52.
- D'ASPREMONT, A., EL GHAOU, L., JORDAN, M. I. and LANCKRIET, G. R. (2007). A direct formulation for sparse PCA using semidefinite programming. *SIAM review* **49** 434–448.
- DINIZ, L. P., ALMEIDA, J. C., TORTELLI, V., VARGAS LOPES, C., SETTI-PERDIGÃO, P., STIPURSKY, J., KAHN, S. A., ROMÃO, L. F., DE MIRANDA, J., ALVES-LEON, S. V., DE SOUZA, J. M., CASTRO, N. G., PANIZZUTTI, R. and GOMES, F. C. A. (2012). Astrocyte-induced synaptogenesis is mediated by transforming growth factor  $\beta$  signaling through modulation of D-serine levels in cerebral cortex neurons. *J Biol Chem* **287** 41432–45.
- FROMER, M., ROUSSOS, P., SIEBERTS, S. K., JOHNSON, J. S., KAVANAGH, D. H., PERUMAL, T. M., RUDERFER, D. M., OH, E. C., TOPOL, A., SHAH, H. R., KLEI, L. L., KRAMER, R., PINTO, D., GUMUS, Z. H., CICEK, A. E., DANG, K., BROWNE, A., LU, C., XIE, L., READHEAD, B., STAHL, E. A., PARVISI, M., HAMAMSY, T., FULLARD, J. F., WANG, Y.-C., MAHAJAN, M. C., DERRY, J. M. J., DUDLEY, J., HEMBY, S. E., LOGSDON, B. A., TALBOT, K., RAJ, T., BENNETT, D. A., DE JAGER, P. L., ZHU, J., ZHANG, B., SULLIVAN, P. F., CHES, A., PURCELL, S. M., SHINOBU, L. A., MANGRAVITE, L. M., TOYOSHIBA, H., GUR, R. E., HAHN, C.-G., LEWIS, D. A., HAROUTONIAN, V., PETERS, M. A., LIPSKA, B. K., BUXBAUM, J. D., SCHADT, E. E., HIRA, K., ROEDER, K.,

- BRENNAND, K. J., KATSANIS, N., DOMINICI, E., DEVLIN, B. and SKLAR, P. (2016). Gene Expression Elucidates Functional Impact of Polygenic Risk for Schizophrenia. *bioRxiv*.
- GU, X., LI, A., LIU, S., LIN, L., XU, S., ZHANG, P., LI, S., LI, X., TIAN, B., ZHU, X. and WANG, X. (2015). MicroRNA124 Regulated Neurite Elongation by Targeting OSBP. *Mol Neurobiol*.
- JOHNSTONE, I. M. and LU, A. Y. (2009). On consistency and sparsity for principal components analysis in high dimensions. *Journal of the American Statistical Association* **104** 682–693.
- JOLLIFFE, I. T., TRENDAFILOV, N. T. and UDDIN, M. (2003). A modified principal component technique based on the LASSO. *Journal of computational and Graphical Statistics* **12** 531–547.
- LEI, J. and VU, V. Q. (2015). Sparsistency and agnostic inference in sparse PCA. *The Annals of Statistics* **43** 299–322.
- LI, J. and CHEN, S. X. (2012). Two sample tests for high-dimensional covariance matrices. *The Annals of Statistics* **40** 908–940.
- MCGRATH, J., SAHA, S., CHANT, D. and WELHAM, J. (2008). Schizophrenia: a concise overview of incidence, prevalence, and mortality. *Epidemiol Rev* **30** 67–76.
- SCHIZOPHRENIA WORKING GROUP OF THE PSYCHIATRIC GENOMICS CONSORTIUM (2014). Biological insights from 108 schizophrenia-associated genetic loci. *Nature* **511** 421–7.
- OWEN, M. J., SAWA, A. and MORTENSEN, P. B. (2016). Schizophrenia. *Lancet*.
- PURCELL, S. M., MORAN, J. L., FROMER, M., RUDERFER, D., SOLOVIEFF, N., ROUSSOS, P., O'DUSHLAINE, C., CHAMBERT, K., BERGEN, S. E., KÄHLER, A., DUNCAN, L., STAHL, E., GENOVESE, G., FERNÁNDEZ, E., COLLINS, M. O., KOMIYAMA, N. H., CHOUDHARY, J. S., MAGNUSSON, P. K. E., BANKS, E., SHAKIR, K., GARIMELLA, K., FENNELLY, T., DEPRISTO, M., GRANT, S. G. N., HAGGARTY, S. J., GABRIEL, S., SCOLNICK, E. M., LANDER, E. S., HULTMAN, C. M., SULLIVAN, P. F., MCCARROLL, S. A. and SKLAR, P. (2014). A polygenic burden of rare disruptive mutations in schizophrenia. *Nature* **506** 185–90.
- RAVASZ, E., SOMERA, A. L., MONGRU, D. A., OLTVAI, Z. N. and BARABÁSI, A.-L. (2002). Hierarchical organization of modularity in metabolic networks. *science* **297** 1551–1555.
- RAVIKUMAR, P., WAINWRIGHT, M. J., RASKUTTI, G., YU, B. et al. (2011). High-dimensional covariance estimation by minimizing 1-penalized log-determinant divergence. *Electronic Journal of Statistics* **5** 935–980.
- SCHOTT, J. R. (2007). A test for the equality of covariance matrices when the dimension is large relative to the sample sizes. *Computational Statistics & Data Analysis* **51** 6535–6542.
- SHEN, H. and HUANG, J. Z. (2008). Sparse principal component analysis via regularized low rank matrix approximation. *Journal of multivariate analysis* **99** 1015–1034.
- SRIVASTAVA, M. S. and YANAGIHARA, H. (2010). Testing the equality of several covariance matrices with fewer observations than the dimension. *Journal of Multivariate Analysis* **101** 1319–1329.
- VERSHYNIN, R. (2010). Introduction to the non-asymptotic analysis of random matrices. *arXiv preprint arXiv:1011.3027*.
- VU, V. Q., CHO, J., LEI, J. and ROHE, K. (2013). Fantope projection and selection: A near-optimal convex relaxation of sparse PCA. In *Advances in Neural Information Processing Systems* **26** 2670–2678.
- WITTEN, D. M., TIBSHIRANI, R. and HASTIE, T. (2009). A penalized matrix decomposition, with applications to sparse principal components and canonical correlation analysis. *Biostatistics* **10** 515–534.
- WU, T.-L. and LI, P. (2015). Tests for High-Dimensional Covariance Matrices Using Random Matrix Projection. *arXiv preprint arXiv:1511.01611*.
- YU, C.-Y., GUI, W., HE, H.-Y., WANG, X.-S., ZUO, J., HUANG, L., ZHOU, N., WANG, K. and WANG, Y. (2014). Neuronal and astroglial TGF $\beta$ 3-Smad3 signaling pathways differentially regulate dendrite growth and synaptogenesis. *Neuromolecular Med* **16** 457–72.
- YUAN, M. (2010). High dimensional inverse covariance matrix estimation via linear programming. *The Journal of Machine Learning Research* **11** 2261–2286.
- ZHANG, B. and HORVATH, S. (2005). A general framework for weighted gene co-expression network analysis. *Statistical applications in genetics and molecular biology* **4** Article17.
- ZOU, H., HASTIE, T. and TIBSHIRANI, R. (2006). Sparse principal component analysis. *Journal of computational and graphical statistics* **15** 265–286.

APPENDIX A: PROOFS UNDER  $L_1$  CONSTRAINTS

*Notations.* For  $Z = (Z_1, \dots, Z_N) = (X_1, \dots, X_n, Y_1, \dots, Y_m)$ , we further define  $Z_{ki}$  to be the  $i$ -th coordinate of the  $k$ -th sample  $Z_k$ , and

$$\hat{\Sigma} = \frac{1}{N} \sum_{k=1}^N Z_k Z_k^T, \quad \bar{Z} = \frac{1}{N} \sum_{k=1}^N Z_k = (\bar{Z}_1, \dots, \bar{Z}_p)^T,$$

$$m_z = \|Z\|_\infty, \quad \bar{m}_z = \|\bar{Z}\|_\infty, \quad \bar{m}_z^{(2q)} = \max_{1 \leq i, j \leq p} \frac{1}{N} \sum_{k=1}^N Z_{ki}^q Z_{kj}^q, \quad q = 1, 2.$$

PROOF OF THEOREM 1. By theorem 2 and lemma 2, we know that there exist constants  $C', C''$  depending on  $(\underline{c}, \bar{c}, \nu^2, \delta)$ , such that after  $(n, p)$  being large enough, with probability at least  $1 - \delta$ ,

$$\|\hat{D}^*\|_\infty \leq C' \sqrt{\frac{\log p}{n}}, \quad \|\hat{D} - D\|_\infty \leq C'' \sqrt{\frac{\log p}{n}}.$$

Then apply theorem 3 on both  $\hat{D}, -\hat{D}$  and  $\hat{D}^*, -\hat{D}^*$ . This together with assumption (A4) imply the desired conclusion with  $C = C' + C''$ .  $\square$

PROOF OF THEOREM 2. First, note that for  $\forall \epsilon > 0$ ,

$$\mathbb{P}\left(\|\hat{D}^*\|_\infty > \epsilon\right) \leq \mathbb{P}\left(\|\hat{\Sigma}_1^* - \hat{\Sigma}\|_\infty > \frac{\epsilon}{2}\right) + \mathbb{P}\left(\|\hat{\Sigma}_2^* - \hat{\Sigma}\|_\infty > \frac{\epsilon}{2}\right). \quad (\text{A.1})$$

Now for any  $\delta > 0$  and constants  $C_1, C_2$ , define

$$\mathcal{A} = \left\{ Z : m_z \leq C_2 \sqrt{\log(C_1 n p / \delta)}, \bar{m}_z \leq C_2 \sqrt{\frac{\log(C_1 p / \delta)}{n}}, \bar{m}_z^{(2q)} \leq C_2, q = 1, 2 \right\}.$$

By lemma 2, there exist constants  $C_1, C_2$  depending on  $(\underline{c}, \bar{c}, \nu^2)$ , such that after  $(n, p)$  being large enough,  $\mathbb{P}(Z \notin \mathcal{A}) \leq \frac{\delta}{4}$ . Therefore, in order to have

$$\mathbb{P}\left(\|\hat{\Sigma}_1^* - \hat{\Sigma}\|_\infty > \frac{\epsilon}{2}\right) \leq \mathbb{P}\left(\|\hat{\Sigma}_1^* - \hat{\Sigma}\|_\infty > \frac{\epsilon}{2} \mid Z \in \mathcal{A}\right) + \mathbb{P}(Z \notin \mathcal{A}) \leq \frac{\delta}{2},$$

it suffices to show that given any  $Z \in \mathcal{A}$ , the conditional probability satisfies

$$\mathbb{P}_Z\left(\|\hat{\Sigma}_1^* - \hat{\Sigma}\|_\infty > \frac{\epsilon}{2}\right) \leq \frac{\delta}{4}. \quad (\text{A.2})$$

For any  $1 \leq i, j \leq p$ , we first bound the  $(i, j)$ -th entry:

$$\mathbb{P}_Z\left(\left|\hat{\Sigma}_{1,ij}^* - \hat{\Sigma}_{ij}\right| > \frac{\epsilon}{2}\right) \leq \mathbb{P}_Z\left(\underbrace{\left|\frac{1}{n} \sum_{k=1}^n Z_{ki}^* Z_{kj}^* - \frac{1}{N} \sum_{k=1}^N Z_{ki} Z_{kj}\right|}_{\Delta_1} > \frac{\epsilon}{4}\right) +$$

$$+ \mathbb{P}_Z\left(\underbrace{\left|\bar{X}_i^* \bar{X}_j^* - \bar{Z}_i \bar{Z}_j\right|}_{\Delta_2} > \frac{\epsilon}{4}\right),$$

where  $\bar{X}_i^* = \frac{1}{n} \sum_{k=1}^n Z_{ki}^*$ . Now we analyze  $\Delta_1, \Delta_2$  separately.

(i) Note that for any  $(k, i, j)$ ,

$$|Z_{ki}^* Z_{kj}^*| \leq (m_z)^2, \quad \text{var}_Z (Z_{ki}^* Z_{kj}^*) \leq \frac{1}{N} \sum_{l=1}^N Z_{li}^2 Z_{lj}^2 \leq \overline{m}_z^{(4)}.$$

Apply lemma 1, there exists constant  $C'_2$  depending on  $(C_2, \nu^2)$ , such that after  $(n, p)$  being large enough,

$$\Delta_1 \leq 2 \exp \left\{ -\frac{n\epsilon^2/C'_2}{1 + \log(C_1 np/\delta)\epsilon} \right\}. \quad (\text{A.3})$$

(ii) Note that

$$\bar{X}_i^* \bar{X}_j^* - \bar{Z}_i \bar{Z}_j = (\bar{X}_i^* - \bar{Z}_i)(\bar{X}_j^* - \bar{Z}_j) + \bar{Z}_j(\bar{X}_i^* - \bar{Z}_i) + \bar{Z}_i(\bar{X}_j^* - \bar{Z}_j),$$

and for any  $(k, i, j)$ ,

$$|\bar{Z}_i| \leq \overline{m}_z, \quad |Z_{ki}^*| \leq m_z, \quad \text{var}_Z (Z_{ki}^*) \leq \frac{1}{N} \sum_{l=1}^N Z_{li}^2 \leq \overline{m}_z^{(2)}.$$

Therefore,

$$\Delta_2 \leq 2 \max_i \left[ \mathbb{P}_Z \left( \left| \frac{1}{n} \sum_{k=1}^n Z_{ki}^* - \bar{Z}_i \right| > \sqrt{\frac{\epsilon}{8}} \right) + \mathbb{P}_Z \left( \left| \frac{1}{n} \sum_{k=1}^n Z_{ki}^* - \bar{Z}_i \right| > \frac{\epsilon}{16\overline{m}_z} \right) \right].$$

Again, apply lemma 1 on both terms, there exists constant  $C''_2$  depending on  $(C_2, \nu^2)$ , such that after  $(n, p)$  being large enough,

$$\begin{aligned} \Delta_2 \leq & 4 \exp \left\{ -\frac{n\epsilon/C''_2}{1 + \sqrt{\log(C_1 np/\delta)}\sqrt{\epsilon}} \right\} + \\ & 4 \exp \left\{ -\frac{n\epsilon^2/C''_2}{\frac{\log(C_1 p/\delta)}{n} + \sqrt{\frac{\log(C_1 p/\delta) \log(C_1 np/\delta)}{n}}\epsilon} \right\}. \end{aligned} \quad (\text{A.4})$$

Combining (A.3) and (A.4), and note that  $(\log p)^3 \leq O(n)$  by assumption (A3), we have  $\Delta_1, \Delta_2 \leq \frac{\delta}{8} p^{-2}$  after  $(n, p)$  being large enough, as long as

$$\epsilon \geq C' \sqrt{\frac{\log(C_1 p^2/\delta)}{n}}$$

for some constant  $C'$  depending on  $C'_2, C''_2$ . Finally, (A.2) follows from a union bound over  $1 \leq i, j \leq p$ . Similar result also holds for  $\|\hat{\Sigma}_2^* - \hat{\Sigma}\|_\infty$  with sample size  $m$ , and the final result follows from (A.1) and the fact that  $\underline{cn} \leq m \leq \bar{cn}$ .  $\square$

**PROOF OF THEOREM 3.** (i) Note that feasible solutions of (2.12) or (2.14) always have  $\|H\|_1 \leq R$ , where  $H = vv^T$  if using (2.14). Then the result directly follows from Hölder's inequality:

$$\text{tr}(\hat{D}H) \leq \|\hat{D}\|_\infty \|H\|_1.$$

- (ii) Let  $v^*$  be the  $R$ -sparse leading eigenvector of  $D$ , then  $\|v^*\|_2 = 1$  and  $\|v^*(v^*)^T\|_1 = \|v^*\|_1^2 \leq \|v^*\|_0 = R$ , so  $v^*(v^*)^T$  is a feasible point in (2.12) and (2.14). The result follows from

$$\tilde{\lambda}_1^R(\hat{D}) - \lambda_1^R(D) \geq (v^*)^T \hat{D} v^* - (v^*)^T D v^*$$

$$\text{and } \left| (v^*)^T (\hat{D} - D) v^* \right| \leq \|\hat{D} - D\|_\infty \|v^*(v^*)^T\|_1.$$

□

LEMMA 1 (Bernstein inequality for sampling without replacement). *Let  $\mathcal{Z} = \{z_1, \dots, z_N\}$  be a finite set containing  $N$  real numbers, and  $(z_1^*, \dots, z_n^*)$  be i.i.d. random variables that are drawn without replacement from  $\mathcal{Z}$ . Let*

$$\bar{z} = \max_{1 \leq i \leq N} |z_i|, \quad \mu_z = \frac{1}{N} \sum_{i=1}^N z_i, \quad \sigma_z^2 = \frac{1}{N} \sum_{i=1}^N (z_i - \mu_z)^2,$$

then for any  $\epsilon > 0$ ,

$$\mathbb{P} \left( \left| \frac{1}{n} \sum_{i=1}^n z_i^* - \mu_z \right| \geq \epsilon \right) \leq 2 \exp \left\{ -\frac{n\epsilon^2}{2\sigma_z^2 + \frac{4}{3}\bar{z}\epsilon} \right\}.$$

As a consequence, for any  $t > 0$ ,

$$\mathbb{P} \left( \left| \frac{1}{n} \sum_{i=1}^n z_i^* - \mu_z \right| > \frac{4\bar{z}}{3} \frac{t}{n} + \sqrt{2\sigma_z^2 \frac{t}{n}} \right) \leq 2e^{-t}.$$

PROOF. See Proposition 1.4 in [Bardenet et al. \(2015\)](#). □

LEMMA 2 (Sub-gaussian tail bound). *Under assumptions (A1)-(A2), for  $\forall \delta > 0$ , there exist constants  $C_1, C_2$  depending on  $(\underline{c}, \bar{c}, \nu^2)$ , such that after  $(n, p)$  being large enough, with probability at least  $1 - \delta$ ,*

$$(i) \quad \|\hat{\Sigma}_q - \Sigma_q\|_\infty \leq C_2 \sqrt{\frac{\log(C_1 p^2 / \delta)}{N}} \text{ for } q = 1, 2. \text{ As a consequence,}$$

$$\|\hat{D} - D\|_\infty \leq 2C_2 \sqrt{\frac{\log(C_1 p^2 / \delta)}{N}}.$$

$$(ii) \quad \bar{m}_z \leq C_2 \sqrt{\frac{\log(C_1 p / \delta)}{N}}. \text{ This together with (i) imply that}$$

$$\bar{m}_z^{(2)} \leq 2\nu^2 + 2C_2 \sqrt{\frac{\log(C_1 p^2 / \delta)}{N}}.$$

$$(iii) \quad m_z \leq C_2 \sqrt{\log(C_1 N p / \delta)}.$$

$$(iv) \quad \bar{m}_z^{(4)} \leq C_2 \left[ 1 + \frac{\log(C_1 p^2 / \delta)}{N} \right].$$

PROOF. (i) See for example, Lemma 12 in Yuan (2010).

- (ii) The first part is standard Hoeffding's bound on  $\frac{1}{N} \sum_{k=1}^N Z_{ki}$ , with a union bound over  $1 \leq i \leq p$ . The second part follows from

$$\overline{m}_z^{(2)} \leq \max\{\|\hat{\Sigma}_1\|_\infty, \|\hat{\Sigma}_2\|_\infty\} + (\overline{m}_z)^2.$$

- (iii) By Markov inequality,  $\forall \epsilon, t > 0$ ,

$$\begin{aligned} \mathbb{P}\left(\max_{k,i} Z_{ki} > \epsilon\right) &\leq e^{-t\epsilon} \mathbb{E}\left[e^{t \max_{k,i} Z_{ki}}\right] = e^{-t\epsilon} \mathbb{E}\left[\max_{k,i} e^{tZ_{ki}}\right] \\ &\leq e^{-t\epsilon} \sum_{k=1}^N \sum_{i=1}^p \mathbb{E}\left[e^{tZ_{ki}}\right] \leq Np \cdot e^{-t\epsilon + \frac{t^2\nu^2}{2}}. \end{aligned}$$

Finally, take  $t = \frac{\epsilon}{\nu^2}$ , and note that similar arguments hold for  $-Z_{ki}$ .

- (iv) For any given  $(i, j)$ , let  $W_k = Z_{ki}^2 Z_{kj}^2$ , and define its cumulant generating function

$$\Psi_k(\theta) = \log \mathbb{E}\left[e^{\theta(W_k - \mathbb{E}(W_k))}\right].$$

Note that  $\Psi_1 = \dots = \Psi_n$  and  $\Psi_{n+1} = \dots = \Psi_{n+m}$ . By Markov inequality, for any  $t, \theta > 0$ ,

$$\mathbb{P}\left(\left|\frac{1}{n} \sum_{k=1}^n W_k - \mathbb{E}(W_1)\right| > t\right) \leq 2 \exp\{-n\theta t + n\Psi(\theta)\}, \quad (\text{A.5})$$

where  $\Psi(\theta) = \max\{\Psi_1(\theta), \Psi_{n+1}(\theta)\}$  is an upper bound of the cumulant generating functions. Since  $Z_{ki}, Z_{kj}$  are sub-gaussian, there exists a small constant  $\theta_0 \neq 0$ , such that  $\Psi(\theta_0) < \infty$ . Plugging in  $\theta_0$  to (A.5), we know that with probability at least  $1 - \frac{\delta}{2}p^{-2}$ ,

$$\frac{1}{n} \sum_{k=1}^n W_k - \mathbb{E}(W_1) \leq \frac{\log(4p^2/\delta)}{n\theta_0} + \frac{\Psi(\theta_0)}{\theta_0}.$$

The same arguments also hold for  $\frac{1}{m} \sum_{k=(n+1)}^{n+m} W_k - \mathbb{E}(W_{n+1})$ . Then the final result follows from a union bound over  $(i, j)$  and the fact that  $\mathbb{E}(W_k) \leq C\nu^4$  for some constant  $C$ . □

## APPENDIX B: PROOFS UNDER $L_0$ CONSTRAINTS

PROOF OF THEOREM 4. By theorem 5 and theorem 6, together with assumption (A3'), we know that for any  $\delta > 0$ , there exist constants  $C_1, C_2, C_3$  depending on  $(\underline{c}, \bar{c}, \nu^2, \delta)$ , such that with probability at least  $1 - \delta$ ,

$$\lambda_1^R(\hat{D}^*) \leq C_1 \sqrt{R \log(C_2 p)/n}, \quad \lambda_1^R(\hat{D}) \geq \lambda_1^R(D) - C_3 \sqrt{1/n}.$$

The same arguments hold for  $-\hat{D}^*$  and  $-\hat{D}$ . Therefore, under assumption (A4') with some constant  $C$  depending on  $(\underline{c}, \bar{c}, \nu^2, \delta)$ , we have

$$\mathbb{P}_{H_1}\left(T_R(\hat{D}^*) > T_R(\hat{D})\right) \leq \delta.$$

The remaining conclusion follows by picking  $\delta = \frac{\alpha}{2}$  and applying standard Hoeffding's bound on the sample mean of Bernoulli random variables.  $\square$

**THEOREM 5** (Permutation test statistic under  $L_0$  constraint). *Let  $\hat{D}^*$  be the permutation differential matrix as defined in (2.9), and  $\lambda_1^R(\hat{D}^*)$  be the exact solution of (2.7). Then under assumptions (A1)-(A2), for any  $\delta > 0$ , there exist constants  $C_1, C_2, C_3$  depending on  $(\underline{c}, \bar{c}, \nu^2)$ , such that with probability at least  $1 - \delta$ ,*

$$\lambda_1^R(\hat{D}^*) \leq h(C_1, C_2, C_3, t),$$

where

$$h(C_1, C_2, C_3, t) = C_1 s [\log(C_3 N p) + t] \frac{t}{N} + C_2 \sqrt{\left(1 + \frac{t + s \log(9ep/s)}{N}\right) \frac{t}{N}},$$

and  $s = \lfloor R \rfloor$ ,  $t = s \log(9ep/s) + \log(1/\delta)$ .

**PROOF.** Following Vershynin (2010), for integer  $s$ , there exists a  $\frac{1}{4}$ -net  $\mathcal{N}_s$  over the unit sphere  $\mathbb{S}^{s-1}$ , such that  $|\mathcal{N}_s| \leq 9^s$ , and for any matrix  $A \in \mathbb{R}^{s \times s}$ ,

$$\lambda_1(A) \leq 2 \max_{v \in \mathcal{N}_s} v^T A v.$$

Now, for any  $\mathcal{S} \subseteq \{1, \dots, p\}$ , denote  $\hat{D}_{\mathcal{S}}^*$  to be the sub-matrix on  $\mathcal{S} \times \mathcal{S}$ , we have

$$\lambda_1^R(\hat{D}^*) = \lambda_1^s(\hat{D}^*) = \max_{|\mathcal{S}|=s} \lambda_1(\hat{D}_{\mathcal{S}}^*) \leq 2 \max_{|\mathcal{S}|=s} \max_{v \in \mathcal{N}_s} v^T (\hat{D}_{\mathcal{S}}^*) v.$$

Moreover, for any given  $v \in \mathcal{N}_s$  and subset  $\mathcal{S}$ , we can construct  $u \in \mathbb{S}^{p-1}$  that is augmented from  $v \in \mathbb{S}^{s-1}$  by adding zeros on coordinates in  $\mathcal{S}^c$ , then

$$v^T (\hat{D}_{\mathcal{S}}^*) v = u^T \hat{D}^* u.$$

We define the collection of such  $u$ 's as

$$\tilde{\mathcal{N}}_s = \{u \in \mathbb{R}^p : \|u\|_2 = 1, \text{supp}(u) \subseteq \mathcal{S}, |\mathcal{S}| = s, u(\mathcal{S}) \in \mathcal{N}_s\},$$

where  $u(\mathcal{S})$  is the sub-vector restricted on coordinates in  $\mathcal{S}$ , and we have

$$|\tilde{\mathcal{N}}_s| = \binom{p}{s} |\mathcal{N}_s| \leq \left(\frac{9ep}{s}\right)^s.$$

Next, we show that there exist constants  $C_1, C_2, C_3$  depending on  $(\underline{c}, \bar{c}, \nu^2)$ , such that

$$\mathbb{P}\left(u^T \hat{D}^* u \geq h\left(\frac{C_1}{2}, \frac{C_2}{2}, C_3, t\right)\right) \leq e^{-t}, \forall t > 0, \forall u \in \tilde{\mathcal{N}}_s. \quad (\text{B.1})$$

Note that

$$u^T \hat{D}^* u = \frac{1}{m} \sum_{l=(n+1)}^N (u^T Z_l^*)^2 - \frac{1}{n} \sum_{k=1}^n (u^T Z_k^*)^2,$$

and we define

$$\gamma_z = \max_{u \in \tilde{\mathcal{N}}_s} \max_{1 \leq k \leq N} Z_k^T u, \quad \bar{\gamma}_z^{(4)} = \max_{u \in \tilde{\mathcal{N}}_s} \frac{1}{N} \sum_{k=1}^N (Z_k^T u)^4,$$

and

$$\mathcal{G} = \left\{ Z : \gamma_z \leq C'_1 \sqrt{s} \sqrt{\log(C'_3 N p)} + t, \quad \bar{\gamma}_z^{(4)} \leq C'_2 \left(1 + \frac{t + s \log(9ep/s)}{N}\right) \right\}.$$

Now for any  $t > 0$ , by lemma 3, there exist constants  $C'_1, C'_2, C'_3$  depending on  $\nu^2$ , such that

$$\mathbb{P}(Z \in \mathcal{G}) \geq 1 - \frac{e^{-t}}{2}.$$

Therefore, in order to prove (B.1), it suffices to show that given any  $Z \in \mathcal{G}$ , the conditional probability satisfies

$$\mathbb{P}_Z \left( \frac{1}{m} \sum_{l=(n+1)}^N (u^T Z_l^*)^2 - \frac{1}{n} \sum_{k=1}^n (u^T Z_k^*)^2 \geq h \left( \frac{C_1}{2}, \frac{C_2}{2}, C_3, t \right) \right) \leq \frac{e^{-t}}{2}.$$

Next, note that given  $Z \in \mathcal{G}$ ,  $(u^T Z_k^*)^2$  satisfies

$$\max_{1 \leq k \leq N} (u^T Z_k^*)^2 \leq (\gamma_z)^2, \quad \text{var}_Z \left[ (u^T Z_k^*)^2 \right] \leq \bar{\gamma}_z^{(4)}, \quad \forall k = 1, \dots, N.$$

Therefore, by lemma 1, there exist constants  $C_1, C_2, C_3$  depending on  $(\nu^2, C'_1, C'_2, C'_3)$ , such that

$$\mathbb{P}_Z \left( \left| \frac{1}{n} \sum_{k=1}^n (u^T Z_k^*)^2 - \frac{1}{N} \sum_{k=1}^N (u^T Z_k)^2 \right| \geq h \left( \frac{C_1}{2}, \frac{C_2}{2}, C_3, t \right) \right) \leq \frac{e^{-t}}{4}.$$

Then (B.1) follows since similar results also hold for  $\frac{1}{m} \sum_{l=(n+1)}^N (u^T Z_l^*)^2$  and  $\underline{cn} \leq m \leq \bar{n}$ . Finally, after applying a union bound over  $\tilde{\mathcal{N}}_s$ , we get for any  $\delta > 0$ ,

$$\begin{aligned} \mathbb{P} \left( \lambda_1^R(\hat{D}^*) > h(C_1, C_2, C_3, t) \right) &\leq \sum_{u \in \tilde{\mathcal{N}}_s} \mathbb{P} \left( u^T \hat{D}^* u > \frac{h(C_1, C_2, C_3, t)}{2} \right) \\ &= \sum_{u \in \tilde{\mathcal{N}}_s} \mathbb{P} \left( u^T \hat{D}^* u > h \left( \frac{C_1}{2}, \frac{C_2}{2}, C_3, t \right) \right) \\ &\leq \left( \frac{9ep}{s} \right)^s e^{-t} = \delta, \end{aligned}$$

where the last equality holds when  $t = s \log(9ep/s) + \log(1/\delta)$ .  $\square$

**THEOREM 6** (Signal under  $L_0$  constraint). *Under assumptions (A1)-(A2), for any  $\delta > 0$ , there exist constants  $C_1, C_2$ , such that with probability at least  $1 - \delta$ ,*

$$\lambda_1^R(\hat{D}) \geq \lambda_1^R(D) - C_1 \frac{\nu^2 \log(2/\delta)}{n} - \sqrt{C_2 \frac{\nu^4 \log(2/\delta)}{n}}.$$

**PROOF.** Let  $u_0 \in B_0(R) = \{u : \|u\|_2 = 1, \|u\|_0 \leq R\}$  such that  $\lambda_1^R(D) = u_0^T D u_0$ . Then

$$\lambda_1^R(\hat{D}) - \lambda_1^R(D) \geq u_0^T (\hat{D} - D) u_0.$$

Therefore, it suffices to bound

$$\left| u_0^T (\hat{D} - D) u_0 \right| \leq \left| u_0^T (\hat{\Sigma}_1 - \Sigma_1) u_0 \right| + \left| u_0^T (\hat{\Sigma}_2 - \Sigma_2) u_0 \right|.$$

Now for any  $\epsilon > 0$ , note that  $X_k^T u_0$  is sub-gaussian for  $\forall k$ , so by standard results (see Lemma 1 in [Ravikumar et al. \(2011\)](#)),

$$\begin{aligned} \mathbb{P} \left( \left| u_0^T (\hat{\Sigma}_1 - \Sigma_1) u_0 \right| > \epsilon \right) &= \mathbb{P} \left( \left| \frac{1}{n} \sum_{k=1}^n (X_k^T u_0)^2 - \mathbb{E} [(X_1^T u_0)^2] \right| > \epsilon \right) \\ &\leq 2 \exp \left\{ - \frac{n \epsilon^2}{C'_1 \nu^4 + C'_2 \nu^2 \epsilon} \right\} \end{aligned}$$

for some constants  $C'_1, C'_2$ . The same arguments hold for  $u_0^T (\hat{\Sigma}_2 - \Sigma_2) u_0$ .  $\square$

**LEMMA 3.** *Under the same conditions as theorem 5, let  $\tilde{\mathcal{N}}_s \subseteq B_0(s) = \{u \in \mathbb{R}^p : \|u\|_2 = 1, \|u\|_0 \leq s\}$  be a finite set such that  $|\tilde{\mathcal{N}}_s| < \infty$ . Define*

$$\gamma_z = \max_{u \in \tilde{\mathcal{N}}_s} \max_{1 \leq k \leq N} Z_k^T u, \quad \bar{\gamma}_z^{(4)} = \max_{u \in \tilde{\mathcal{N}}_s} \frac{1}{N} \sum_{k=1}^N (Z_k^T u)^4.$$

*Then for any  $t > 0$ , there exist constants  $C_1, C_2, C_3$  depending on  $\nu^2$ , such that with probability at least  $1 - e^{-t}$ ,*

$$\gamma_z \leq C_1 \sqrt{s} \sqrt{\log(C_3 N p)} + t, \quad \bar{\gamma}_z^{(4)} \leq C_2 \left[ 1 + \frac{t + \log |\tilde{\mathcal{N}}_s|}{N} \right].$$

**PROOF.** Let  $m_z = \|Z\|_\infty = \max_{1 \leq k \leq N, 1 \leq j \leq p} Z_{kj}$ , and note that

$$\gamma_z = \max_{u \in \tilde{\mathcal{N}}_s} \max_{1 \leq k \leq N} Z_k^T u \leq m_z \cdot \max_{u \in \tilde{\mathcal{N}}_s} \sum_{j=1}^s u_j \leq m_z \sqrt{s}.$$

Then the first result follows from lemma 2.

Next, for any  $u \in \tilde{\mathcal{N}}_s$ , denote  $W_{u,k} = (Z_k^T u)^4$ , with cumulant generating function

$$\Psi_k(\theta) = \log \mathbb{E} \left[ e^{\theta [W_{u,k} - \mathbb{E}(W_{u,k})]} \right].$$

Note that  $\Psi_1 = \dots = \Psi_n$  and  $\Psi_{n+1} = \dots = \Psi_{n+m}$ . Then for any  $\epsilon, \theta > 0$ , by Markov inequality,

$$\mathbb{P} \left( \frac{1}{N} \sum_{k=1}^N (W_{u,k} - \mathbb{E}(W_{u,k})) > \epsilon \right) \leq \exp \{-N\theta\epsilon + N\Psi(\theta)\}, \quad (\text{B.2})$$

where  $\Psi(\theta) = \max\{\Psi_1(\theta), \Psi_{n+1}(\theta)\}$ . Since  $\{W_{u,k}\}_{k=1, \dots, N}$  are sub-gaussian, there exists a small constant  $\theta_0 \neq 0$ , such that  $\Psi(\theta_0) < \infty$ . Therefore, plugging  $\theta_0$  into (B.2), we know that with probability at least  $1 - e^{-t}/|\tilde{\mathcal{N}}_s|$ ,

$$\frac{1}{N} \sum_{k=1}^N (W_{u,k} - \mathbb{E}(W_{u,k})) \leq \frac{t + \log |\tilde{\mathcal{N}}_s|}{N\theta_0} + \frac{\Psi(\theta_0)}{\theta_0}.$$

Finally, the desired result follows from a union bound over  $u \in \tilde{\mathcal{N}}_s$  and the fact that  $\mathbb{E}(W_{u,k}) \leq C\nu^4$  for some constant  $C$ .  $\square$